◆ Human Brain Mapping 35:3332–3342 (2014) ◆

Idiopathic-Generalized Epilepsy Shows Profound White Matter Diffusion—Tensor Imaging Alterations

Niels K. Focke,[1,2]* Christine Diederich,[1] Gunther Helms,[3] Michael A. Nitsche,[1] Holger Lerche,[2] and Walter Paulus[1]

[1]*Department of Clinical Neurophysiology, Georg-August University, Göttingen, Germany*
[2]*Department of Neurology and Epileptology, Hertie Institute of Clinical Brain Research, University of Tübingen, Tübingen, Germany*
[3]*Department of Cognitive Neurology, MR-Research in Neurology and Psychiatry, Georg-August University, Göttingen, Germany*

Abstract: *Objectives:* Idiopathic-generalized epilepsy (IGE) is currently considered to be a genetic disease without structural alterations on conventional MRI. However, voxel-based morphometry has shown abnormalities in IGE. Another method to analyze the microstructure of the brain is diffusion-tensor imaging (DTI). We sought to clarify which structural alterations are present in IGE and the most frequent subsyndrome juvenile myoclonic epilepsy (JME). *Experimental design:* We studied 25 patients (13 IGE and 12 JME) and 44 healthy controls with DTI. Fractional anisotropy (FA), mean diffusivity (MD), axial and radial diffusivity (AD/RD) were calculated and group differences were analyzed using tract-based spatial statistics (TBSS). Additionally we performed a target-based classification of TBSS results based on the Freesurfer cortical regions. *Principle observations:* TBSS showed widespread FA reductions as well as MD and RD increases in patients compared to controls. Affected areas were corpus callosum, corticospinal tract, superior and inferior longitudinal fasciculus and supplementary motor regions. No significant differences were found between JME and IGE subgroups. The target-based classification confirmed a particular involvement of the superior frontal gyrus (mesiofrontal area) in IGE/ME. *Conclusions:* IGE and JME patients showed clear microstructural alterations in several large white matter tracts. Similar findings have been reported in rodent models of IGE. Previous, region-of-interest-based DTI studies may have under-estimated the spatial extent of structural loss associated with generalized epilepsy. The comparison of clinically defined JME and IGE groups revealed no significant DTI differences in our cohort. *Hum Brain Mapp 35:3332–3342, 2014.* © **2013 Wiley Periodicals, Inc.**

Key words: idiopathic-generalized epilepsy; juvenile myoclonic epilepsy; MRI; diffusion-tensor imaging; fiber tracking

Additional Supporting Information may be found in the online version of this article.

Contract grant sponsors: University Medical Center Göttingen, (Rückkehrer-Startförderung) (to N.K.F.).

*Correspondence to: Niels K. Focke, Department of Neurology and Epileptology, University of Tübingen, 72076 Tübingen, Germany. E-mail: niels.focke@uni-tuebingen.de

Received for publication 5 December 2012; Revised 13 August 2013; Accepted 9 September 2013.

DOI 10.1002/hbm.22405

Published online 6 November 2013 in Wiley Online Library (wileyonlinelibrary.com).

INTRODUCTION

Idiopathic-generalized epilepsy (IGE) is a summary term commonly used to classify patients with a presumed genetic cause of epilepsy and predominantly primarily generalized seizures. Although the most recent 2009 ILAE classification has abandoned the classical terms "generalized" versus "focal" epilepsies in favor for a more etiological concept ("genetic" versus "structural/metabolic") the term IGE is still commonly used in clinical practice [Berg et al., 2010]. A specific, electro-clinically defined subsyndrome of IGE is juvenile myoclonic epilepsy (JME) originally proposed by Janz [1985]. Although by concept the routine MRI is usually normal in IGE and JME, several studies have shown subtle structural abnormalities at the group level using advanced post-processing methods, e.g., voxel-based morphometry (VBM). In JME, these include mesiofrontal increases of gray matter [Betting et al., 2006; Woermann et al., 1999], reduced thalamic volumes [Helms et al., 2006; Kim et al., 2007], alterations of prefrontal MR spectroscopy [Savic et al., 2000] and reduced white matter anisotropy using diffusion-tensor imaging (DTI) in preselected large fiber bundles [Liu et al., 2011; Vulliemoz et al., 2011]. A recent voxel-based DTI study in JME confirmed reduced anisotropy in the corpus callosum [O'Muircheartaigh et al., 2011]. However, the same study reports reduced mesiofrontal gray matter volumes, which contradict previous VBM findings. Studies in IGE with isolated generalized tonic-clonic seizures, another IGE subsyndrome, have shown widespread gray matter volume loss [Ciumas and Savic, 2006; Huang et al., 2011], reduced cortical thickness [Bernhardt et al., 2009] or were negative [Betting et al., 2006].

Although JME is clinically clearly defined, we know very little about the etiology of the disease or if relevant structural differences exists between JME and other IGE subsyndromes. To this end we conducted a study of high-resolution DTI in a single sample of clinically defined JME and IGE patients comparing both groups with each other and with healthy controls. To overcome potential limitations of previous region-based studies we used a whole brain DTI method (tract-based spatial statistics, TBSS). Additionally, we sought to analyze which anatomically defined cortical networks are involved by applying target-based classification of TBSS findings.

METHODS

Patients

We included 25 patients with the clinical diagnosis of IGE or JME (13 IGE and 12 JME) and 44 healthy controls. Six of 13 IGE patients, 6/12 JME patients, and 23/44 controls were women. The mean age was 30.2 (±11.2) years [median 25, interquartile range (IQR) 21] for IGE, 33.1 (±7.5) years for JME (median 34, IQR 13.25) and 31.9 (±8.2) years (median 30, IQR 8.5) for controls. Eight of 13 IGE patients and 4/12 JME patients were seizure free at the time of enrolment. The mean age of onset was 17.1 (±6.4) years (median 16.5, IQR 5.75) for JME and 14.8 (±5.1) years (median 15, IQR 7) for IGE. Mean duration of epilepsy was 16.0 (±11.0) years (median 13.5, IQR 16.75) for JME and 15.5 (±12.3) years (median 11, IQR 18.5) for IGE. There were no significant differences (all $P > 0.3$) between the IGE, JME or control group concerning sex, seizure freedom (chi-square test), age, duration of epilepsy or age of onset (all *t*-test). It is of note that in our cohort the seizure free rate (12/25 = 48%) was lower than what would be expected in unselected patients with generalized epilepsy [Kwan and Brodie, 2000]. Detailed clinical parameters are shown in Supporting Information Table 1. The syndrome definition of JME versus IGE was done clinically according to the treating physician's best judgment. As such all patients without the typical hallmarks of JME, in particular myoclonic jerks (impulsive petit mal), were classified as IGE. We routinely apply video-EEG (usually 48 h recordings) if the syndrome definition based on semiology and routine EEG is unclear. All subjects gave written informed consent; the study was approved by the local ethics committee.

MR Imaging

MRI was performed on a 3T whole-body MRI system (Magnetom Tim Trio, Siemens Healthcare, Erlangen, Germany) using an eight-channel head array coil (Invivo, Gainesville, FA) for signal reception and the body coil for transmission.

We acquired two volumes of a T1-weighted, 3D magnetization-prepared rapid gradient-echo (3D-MPRAGE, TI = 900 ms, $\alpha = 9°$, TE = 3.0–3.2 ms, TR = 2250 ms, 1 mm isotropic resolution) MRI. These were coregistered (second scan rigidly coregistered to first scan) and averaged with the FMRIB Software Library (FSL, version 4.1) (http://www.fmrib.ox.ac.uk/fsl). DTI was measured with an echo planar 2D sequence (2D-EPI, $\alpha = 90°$, TE = 93 ms, TR = 10,000 ms, 1.9 mm isotropic resolution) acquiring 30 image volumes with diffusion-weighting (along 30 noncollinear diffusion directions, B1 images, $b = 1000$ s/mm^2) and 1 reference without diffusion weighting (B0 image). The original DICOM images were transferred to a Linux-based server and converted to 3D NIFTI format using mriconvert (http://lcni.uoregon.edu~jolinda/MRIConvert).

Freesurfer Preprocessing

The averaged T1-weighted volume was processed with Freesurfer v5.1.0 (http://surfer.nmr.mgh.harvard.edu) including bias optimization for 3 T images (recon-all with nuintensitycor-3 T option). The processing yields 150 distinct, atlas-based cortical gray matter labels (aparc.a2009s atlas) [Destrieux et al., 2010] and estimates of the pial and white matter surface. To facilitate tracking and reduce the potential confound of gray matter volume differences the

regions were projected onto the white matter surface and re-converted to a NIFTI volume image. This procedure results in one-dimensional "ribbons" located at the gray matter/white matter junction zone. We considered all 148 cortical Freesurfer regions (excluding the noncortical, zero thickness "medial wall" region) [Destrieux et al., 2010].

DTI Preprocessing

The DTI data were processed with the FSL diffusion tool (FDT). First, each diffusion weighted volume was affinely registered to the $b = 0$ reference volume to correct for eddy currents and slight movements during the acquisition ("eddy-correct" tool). Next, maps of fractional anisotropy (FA) and mean diffusivity (MD) were calculated using "dtifit." We also calculated axial diffusivity (AD), which is the first (principal) eigenvalue, and radial diffusivity (RD), which is the average of the second and third eigenvalue. Preprocessing for probabilistic tractography was done with "bedpostx" estimating two fibers per voxel.

TBSS Analysis

To assess group level differences in the FA and MD maps we applied tract-based spatial statistics (TBSS) [Smith et al., 2007]. For details of the TBSS procedure please refer to the TBSS publication [Smith et al., 2007] or the FSL webpage (http://www.fmrib.ox.ac.uk/fsl/tbss/index.html). In brief, this method generates a pseudo-anatomical "skeleton" from the FA images of all subjects and projects the FA or MD values into this analysis space. Compared to full-brain voxel-based analysis this improves spatial normalization, reduces the multiple comparisons problem and results in higher sensitivity [Focke et al., 2008]. However, by concept the analysis is restricted to white matter. Group differences were analyzed with non-parametric, permutation-based inference using "randomize" with 5,000 permutations and corrected for multiple comparisons at the cluster-level with TFCE (Threshold-Free Cluster Enhancement) and a $P < 0.01$ (corrected for multiple comparisons) threshold. Resulting statistical maps were overlaid on the averaged FA or MD maps of all subjects with MRIcron (http://www.cabiatl.com/mricro/mricron/index.html) for visualization. Additional 3D renderings were done with 3D-Slicer v4.1.0 (http://www.slicer.org/). For reporting purposes, clusters (i.e., connected suprathreshold voxels) were determined with FSL "cluster," subclusters (local maxima within a unique cluster at least 8-mm apart) were also listed. For each cluster and subcluster the peak level (=lowest P value) MNI coordinate (in mm) was identified and anatomically localized using the FSL atlas tools ("JHU White-Matter Tractography Atlas" or, if the former did not find a label, "JHU ICBM-DTI-81 White-Matter Labels"). For conciseness only the 10 most significant (i.e., lowest P value) subclusters were listed in the final table. AD and RD maps were analyzed, respectively, for the combined comparison of IGE and JME versus controls.

Target-Based Classification of TBSS Results

Based on the TBSS detected FA differences of the combined patient group we did a target-based classification of all suprathreshold voxels and the 148 cortical Freesurfer regions. To this end, the thresholded TBSS mask ($P < 0.99$, corrected) was back-projected to each individual's (patient and control) native DTI space ("tbss_deproject," nearest neighbor interpolation). Each TBSS voxels was used as seeds for probabilistic tracking and then classified according to highest connection probability between the seed and the 148 cortical regions ("find_the_biggest") [Behrens et al., 2003]. Next this classified mask was re-projected to the common TBSS skeleton (nearest neighbor interpolation), yielding a distinct, classified TBSS mask per subject. We then calculated the modal value, i.e., most frequent label per voxel, in Matlab resulting in a hard segmentation of the TBSS results. For better visualization the number of voxels was counted for each label and projected onto the respective region of the default Freesurfer subject "bert."

RESULTS

The TBSS analysis showed widespread FA reduction and MD/RD increase in IGE/JME. Detailed results of FA alterations are shown in Table I and Table II, overlay images in Figure 1 and 3D rendering in Figure 2. Detailed MD differences are shown in Supporting Information Table II.

IGE and JME Versus Controls

The statistically most significant DTI alterations were found in the joint analysis of JME and IGE patients compared to controls. Even at a conservative statistical threshold of $P < 0.01$ (corrected) the FA reductions merged into one single cluster with 32,076 suprathreshold voxels corresponding to 22.3% of the entire TBSS skeleton. The analysis of local maxima revealed the most significant reductions in the corpus callosum ($P = 0.001$), the corticospinal tract ($P = 0.001$), the superior longitudinal fasciculus ($P = 0.001$) and white matter of the supplementary motor region ($P = 0.002$). Large areas of the frontal and parietal lobes as well as temporal and occipital lobes were also involved. The analysis of MD changes revealed a similar pattern of increased MD in patients, again with a single widespread cluster of 25,621 supra-threshed voxels. The most significant increases were in the right pericallosal area ($P = 0.007$), the right corticospinal tract ($P = 0.008$), the right anterior thalamic radiation ($P = 0.008$), the corpus callosum ($P = 0.009$) and the superior and inferior fronto-occipital fasciculus (left: $P = 0.009$/right: $P = 0.010$).

TABLE I. FA results

#	*P*	Voxels	*X*	*Y*	*Z*	Atlas
				IGE < controls		
7	0.003	6,368	−17	−26	32	Body of corpus callosum
7	0.004		−20	−34	53	Corticospinal tract L
7	0.004		−20	−25	48	Corticospinal tract L
7	0.004		−22	−45	38	Superior longitudinal fasciculus L
7	0.004		−19	−22	37	Corticospinal tract L
7	0.004		−17	−12	36	Body of corpus callosum
7	0.004		−17	12	35	Superior corona radiata L
7	0.004		−18	−35	35	Cingulum (cingulate gyrus) L
7	0.004		−15	0	34	Body of corpus callosum
7	0.004		−11	−15	30	Body of corpus callosum
7	0.004		−14	−26	29	Body of corpus callosum
7	0.004		11	−18	28	Body of corpus callosum
				[. . .] plus 58 additional subclusters		
6	0.009	43	−29	2	−34	Cingulum (hippocampus) L
6	0.01		−35	−1	−29	Inferior longitudinal fasciculus L
5	0.009	35	−31	−64	35	(Parietal lobe L)
5	0.01		−30	−62	38	(Parietal lobe L)
5	0.01		−34	−68	31	Inferior longitudinal fasciculus L
4	0.01	16	−30	−83	16	Inferior longitudinal fasciculus L
3	0.01	10	−29	−77	12	Inferior longitudinal fasciculus L
2	0.01	9	−33	−79	16	Inferior longitudinal fasciculus L
1	0.01	2	−34	−67	26	(Parietal lobe L)
				IGE > controls		
				No significant differences		
				JME < controls		
5	0.001	11,507	8	−19	26	Body of corpus callosum
5	0.002		25	−21	34	Corticospinal tract R
5	0.002		23	−43	34	Superior longitudinal fasciculus R
5	0.002		−15	9	30	Body of corpus callosum
5	0.002		13	4	30	Body of corpus callosum
5	0.002		−14	−23	30	Body of corpus callosum
5	0.002		15	13	29	Body of corpus callosum
5	0.002		11	−4	29	Body of corpus callosum
5	0.002		26	−34	29	Superior longitudinal fasciculus R
5	0.002		16	−35	29	Splenium of corpus callosum
5	0.002		10	−16	28	Body of corpus callosum
5	0.002		−9	−17	27	Body of corpus callosum
				[. . .] plus 122 additional subclusters		
4	0.008	1,521	27	10	24	Superior corona radiata R
4	0.008		25	12	34	(Frontal lobe R)
4	0.008		30	3	30	Superior longitudinal fasciculus R
4	0.008		29	22	27	(Frontal lobe R)
4	0.008		27	29	22	Anterior thalamic radiation R
4	0.009		23	0	34	Superior corona radiata R
4	0.009		37	2	26	Superior longitudinal fasciculus (temporal part) R
4	0.009		29	27	14	Inferior fronto-occipital fasciculus R
4	0.009		30	37	12	Anterior thalamic radiation R
4	0.009		37	32	11	Inferior fronto-occipital fasciculus R
4	0.009		33	48	7	Anterior thalamic radiation R
				[. . .] plus 10 additional subclusters		
3	0.009	253	32	−1	17	Superior longitudinal fasciculus R
3	0.01		28	−9	26	Corticospinal tract R
3	0.01		35	−3	22	Superior longitudinal fasciculus R
3	0.01		27	−2	20	Superior longitudinal fasciculus R
3	0.01		33	4	18	Superior longitudinal fasciculus R

TABLE I. (continued).

#	*P*	Voxels	*X*	*Y*	*Z*	Atlas
2	0.009	95	19	33	27	Forceps minor
2	0.01		19	24	32	(Frontal lobe R)
2	0.01		21	34	27	Forceps minor
2	0.01		22	40	20	Anterior thalamic radiation R
1	0.01	19	18	47	20	Forceps minor
1	0.01		18	45	21	Forceps minor
				JME > controls		
				No significant differences		
				JME + IGE < controls		
1	0.001	32,076	3	−27	23	Body of corpus callosum
1	0.001		−21	−47	38	Superior longitudinal fasciculus L
1	0.001		−19	−22	37	Corticospinal tract L
1	0.001		−19	−33	35	Posterior corona radiata L
1	0.001		−15	−28	30	Body of corpus callosum
1	0.001		14	−26	29	Anterior thalamic radiation R
1	0.001		−6	−13	26	Body of corpus callosum
1	0.001		3	−14	25	Body of corpus callosum
1	0.001		−7	−24	25	Body of corpus callosum
1	0.002		−6	−10	63	(White matter of the supplementary motor area L)
1	0.002		−11	−2	62	(White matter of the supplementary motor area L)
				[. . .] plus 339 additional subclusters		
				JME + IGE > controls		
				No significant differences		
				JME > IGE		
				No significant differences		
				JME < IGE		
				No significant differences		

Detected clusters of significant ($P < 0.01$, corrected) FA differences. For each cluster (unique cluster index = #) the 10 most significant subclusters (local maxima with a minimal distance of 8 mm) are also listed. The anatomical position was estimated using the "JHU White-Matter Tractography Atlas" supplied with FSL. When no label was found in the former, the "JHU ICBM-DTI-81 White-Matter Labels" atlas was used instead. When both atlases reported no anatomical label a visual assessment was done, these labels are printed in brackets. L = left, R = right, WM = white matter, *P* = corrected *P* value, voxels = number of voxels in this cluster, *X*, *Y*, *Z* = coordinates in MNI space (mm).

To further scrutinize the diffusion characteristics we repeated the TBSS analysis for AD and RD. For RD a very large cluster of 35,851 voxels was detected encompassing the corticospinal tract ($P = 0.001$), the white matter of the supplementary motor area ($P = 0.001$), the superior longitudinal fasciculus ($P = 0.001$) and other regions including large parts of the corpus callosum and all cerebral lobes. The distribution was very similar to the detected FA decrease in patients. For AD no significant differences between patients and controls were found.

IGE Versus Controls

In the IGE group FA reductions had an asymmetrical pattern with more widespread reductions on the left side. Again, suprathreshold voxels formed one large cluster with 6,348 voxels and more than 60 local maxima. The most significant reductions were detected in the corpus callosum ($P = 0.003$), the left corticospinal tract ($P = 0.004$), left superior longitudinal fasciculus ($P = 0.004$), and the left cingulum ($P = 0.004$). The MD analysis confirmed increased values in patients in the corpus callosum ($P = 0.007$), right anterior thalamic radiation ($P = 0.008$), the left cingulum ($P = 0.008$) and the inferior ($P = 0.009$) and superior longitudinal fasciculus ($P = 0.009$).

JME Versus Controls

When the JME group was separately compared to controls, we again found widespread FA reductions. These formed another large cluster with 11,507 voxels. Highest significances of local maxima were found in the corpus callosum ($P = 0.001$), the corticospinal tract ($P = 0.002$) and the right superior longitudinal fasciculus ($P = 0.002$). Changes in general had an emphasis on the frontal lobe and a symmetrical pattern. In contrast, MD increases were weaker with only few supra-threshold voxels in the frontal lobe including the right forceps minor ($P = 0.009$), right anterior thalamic radiation ($P = 0.009$) and inferior fronto-occipital fasciculus ($P = 0.01$).

TABLE II. TBSS RD and AD results

#	*P*	Voxels	*X*	*Y*	*Z*	Atlas
				RD: JME + IGE < controls		
				No significant differences		
				RD: JME+IGE > controls		
1	0	35,851	−41	−37	5	Superior longitudinal fasciculus (temporal part) L
1	0.001		9	−41	64	(Precentral gyrus R)
1	0.001		−12	−27	62	Corticospinal tract L
1	0.001		17	−22	61	Corticospinal tract R
1	0.001		15	−37	59	Corticospinal tract R
1	0.001		−11	−34	58	(Precentral gyrus L)
1	0.001		15	−9	56	(White matter of the supplementary motor area R)
1	0.001		15	−28	56	Corticospinal tract R
1	0.001		−18	−41	56	Corticospinal tract L
1	0.001		21	−49	56	Superior longitudinal fasciculus R
1	0.001		−15	−9	54	(White matter of the supplementary motor area L)
1	0.001		14	7	52	(White matter of the supplementary motor area R)
				[. . .] plus 402 additional subclusters		
				AD: JME + IGE < controls		
				No significant differences		
				AD: JME + IGE > controls		
				No significant differences		

Detected clusters of significant ($P < 0.01$, corrected) RD or AD differences. For each cluster (unique cluster index = #) the 10 most significant subclusters (local maxima with a minimal distance of 8 mm) are also listed. The anatomical position was estimated using the "JHU White-Matter Tractography Atlas" supplied with FSL. When no label was found in the former, the "JHU ICBM-DTI-81 White-Matter Labels" atlas was used instead. When both atlases reported no anatomical label a visual assessment was done, these labels are printed in brackets. L = left, R = right, WM = white matter, *P* = corrected *P* value, voxels = number of voxels in this cluster, *X*, *Y*, *Z* = coordinates in MNI space (mm).

JME Versus IGE

The comparison of JME versus IGE showed no significant differences both for FA as well as for the MD analysis. Even with an exploratory statistical threshold of $P < 0.001$ (uncorrected for multiple comparisons) no significant voxels were found.

Target-Based Classification of TBSS Results

Twenty-two percent of all suprathreshold TBSS voxels (FA, IGE/JME < controls) were classified to be connected to the superior frontal gyrus (11.2% left, 10.8% right). The precentral gyrus was connected to 5.2% of voxels (2.7% left, 2.5% right) followed by the angular part of the inferior parietal gyrus with 4.9% (2.3% left, 2.6% right) and the superior temporal sulcus with 4.6% (2.0% left, 2.6% right). Details are listed in the Supporting Information Table 3. A surface rendering of the connected regions and an overview histogram is shown in Figure 3.

DISCUSSION

Structural Correlates of Generalized Epilepsy

Currently, generalized epilepsies are regarded as genetically defined syndromes without clear structural correlate and usually normal routine brain MRI. However, early neuropathological studies in the mid-1980 have already shown that generalized epilepsy displays specific structural alterations [Meencke, 1985; Meencke and Janz, 1984]. These include "microdysgenesis," a subtle disruption of cortical lamination and increased neuron density while cortical volumes remain normal. Given the ex vivo nature of autopsy studies, the authors could not differentiate whether these were cause or consequence of epilepsy. Recent techniques like VBM allow an in vivo analysis of brain morphology in IGE. However, the observed gray matter differences are controversial. Some authors found increased gray matter volume/density in mesiofrontal areas [Betting et al., 2006; Kim et al., 2007; Woermann et al., 1999]. Other studies found reduced volumes in the same regions [Bernhardt et al., 2009; Liu et al., 2011; O'Muircheartaigh et al., 2011]. Whereas VBM results are contradictory, DTI alterations in IGE are so far relatively consistent. A reduced FA has been found in the white matter of the supplementary motor area in JME patients that was not present in patients with frontal lobe epilepsy [Vulliemoz et al., 2011]. Another study described reduced FA in several large white matter tracts including the corpus callosum in JME [Liu et al., 2011], notably the authors found no FA differences in their group of 10 IGE patients (with generalized tonic-clonic seizures). A reduced FA in the corpus callosum of JME patients has also been

reported in a voxel-based DTI study [O'Muircheartaigh et al., 2011]. Our results confirm these findings; however, we found a similar reduction of FA in undifferentiated IGE as well. Moreover, FA reductions were not limited to the corpus callosum or selected white matter tracts but involved large parts of the TBSS skeleton including the white matter of the supplementary motor area, the corticospinal tract and the superior and inferior longitudinal fasciculus. In the joint analysis of JME and IGE all lobes were involved. These widespread findings indicate that previous, region-based studies may have underestimated the spatial extent of alterations.

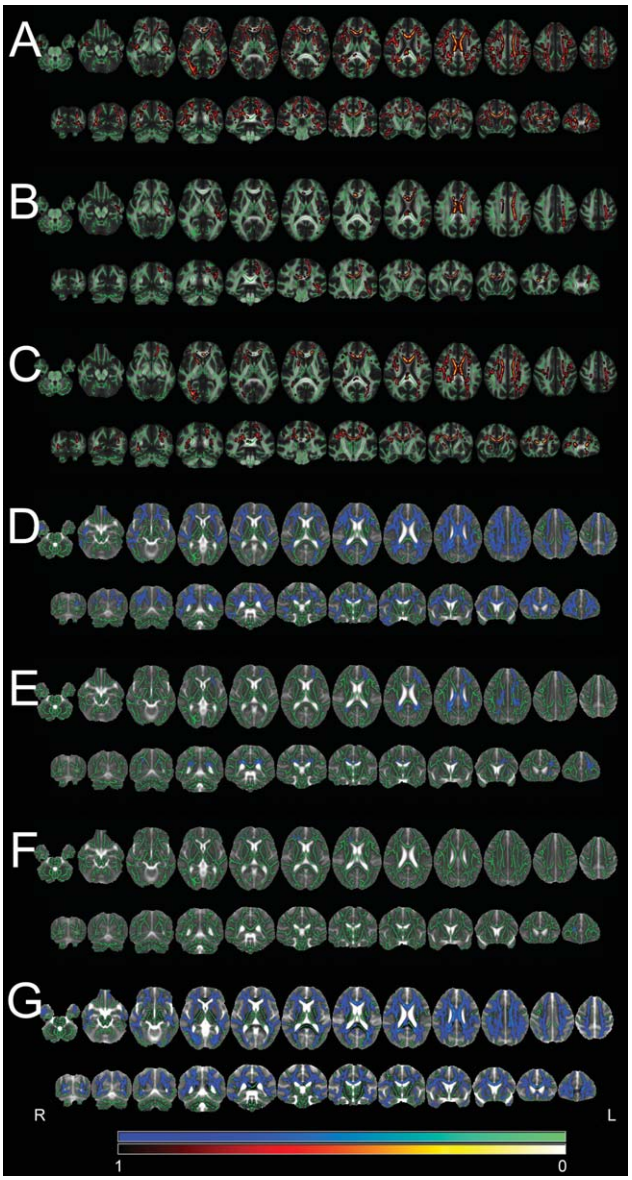

The target-classification approach revealed a region-specific pattern with a particular emphasis on the superior frontal gyrus. This is anatomically concordant to the VBM findings showing mesiofrontal changes (although controversial in terms of gray matter increase or decrease), the "microdysgenesis" described in the frontal lobe histopathologically [Meencke, 1985] and a region-based DTI study [Vulliemoz et al., 2011]. Other affected cortical regions were the precuneus, precentral gyrus and cingulate gyri. These results motivate further studies of network (dys-) function in generalized epilepsy, e.g., graph theory-based approaches.

It is possible that our cohort recruited at a university referral center, was biased towards more refractory patients. In fact only 12 of 25 patients were controlled by medication, which is much lower than the percentage expected in an unselected cohort [Kwan and Brodie, 2000]. Thus, the observed effect size in our sample may be higher than in other, less refractory cohorts. A similar decrease of FA in the corpus callosum and other tracts has been described in different animal models of generalized epilepsy [Jones et al., 2011] and was developmentally linked to seizure evolution and severity [Chahboune et al., 2009]. Thus, this pattern may be a hallmark of generalized epilepsy and an interesting biomarker for epileptogenesis in these patients.

In addition to the analysis of FA and MD DTI parameters, we repeated the TBSS and regional tracking based on axial diffusivity (AD), a putative marker for axonal integrity, and radial diffusivity (RD), a putative marker for myelination [Alexander et al., 2007; Song et al., 2005]. TBSS confirmed that the observed alterations in IGE are predominately associated with increased RD. This infers that a reduced myelination or demyelination may play a role in the pathophysiology of IGE. However, these DTI measures have to be interpreted with caution, should not be mistaken for histopathological proof of myelin loss, be confirmed with other measures

Figure 1.

TBSS results. Significant differences for FA and MD ($P < 0.01$, corrected) as detected by the TBSS analysis are shown overlaid on the skeleton and the averaged FA/MD map. The color scale represents corrected *P* values. Note that for better visibility the significant areas are expanded beyond the original skeleton with tbss_fill after statistical thresholding. "Hot" colors indicate decreases (patients < controls), "cool" colors indicate increases (patients > controls). Left in the images is right in the subjects (radiological convention). **A**: FA differences for patients (JME and IGE combined) versus controls. **B**: FA differences for IGE patients versus controls. **C**: FA differences for JME patients versus controls. **D**: MD differences for patients (JME and IGE combined) versus controls. **E**: MD differences for IGE patients versus controls. **F**: MD differences for JME patients versus controls. **G**: RD differences for patients (JME and IGE combined) versus controls.

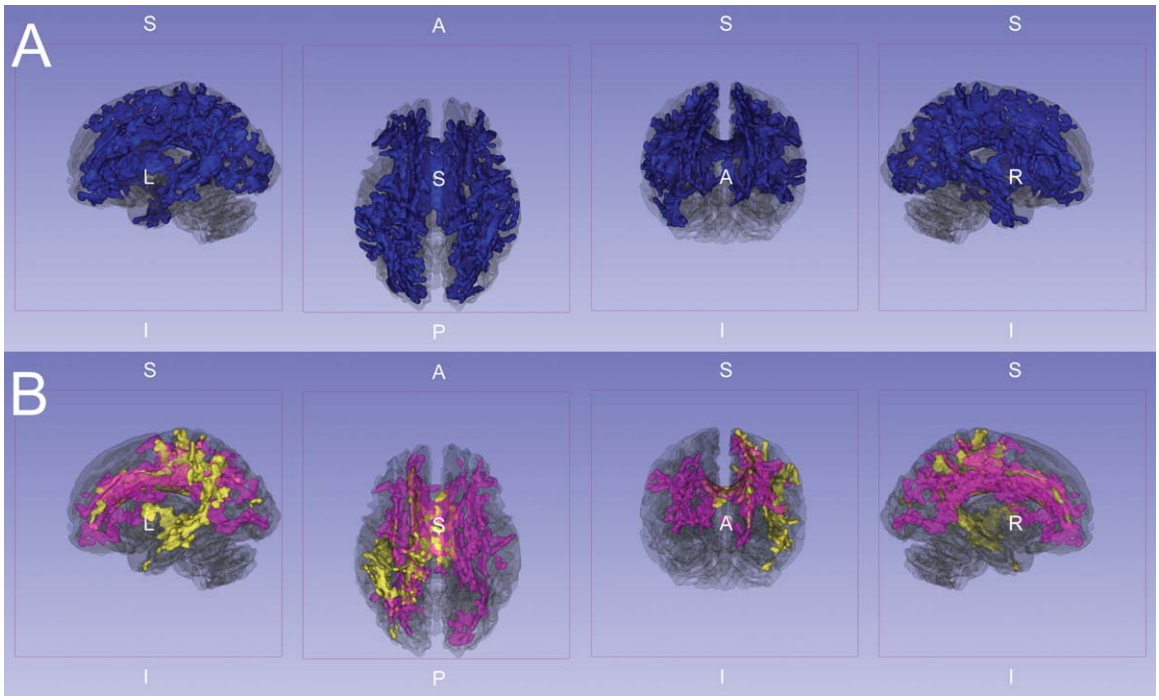

Figure 2.

Three-dimensional rendering of significant FA reductions. This image shows significant ($P < 0.01$, corrected) FA reductions superimposed on the partially transparent white matter skeleton. **A**: IGE and JME jointly compared to controls (blue). **B**: IGE (yellow) and JME (purple) separately compared to controls. Note the differential but overlapping reductions compared to controls in (B). However, when directly compared there were no significant DTI differences between the IGE and JME groups after whole brain error correction ($P > 0.05$ FWE corrected).

and may be subject to technical limitations [Wheeler-Kingshott and Cercignani, 2009]. Our cross-sectional data does not allow to differentiate if these changes indicate a structural loss or a pre-existing, i.e. developmental condition in IGE/JME patients. For patients with mesiotemporal epilepsy a relation of DTI alterations and hippocampal volumes has been shown [Bonilha et al., 2010]. A reduction of myelin without axonal damage would be well concordant with preserved neuronal cell density/cortical volumes as indicated by histopathology [Meencke, 1985; Meencke and Janz, 1984] and inconsistent VBM findings without clear cortical atrophy in generalized epilepsy. However, further studies are needed to investigate this in more detail.

Differentiation of IGE Subsyndromes

None of the methods applied in the present study showed a relevant group difference between clinically defined JME and IGE patients. In fact, when combining the IGE and JME groups, effect sizes were higher indicating that an increased power due to sample size outweighs syndrome-specific effects. Hence, on a structural basis, the differences between JME and undifferentiated IGE appear limited. A VBM study done in different IGE subsyndromes (JME, absence epilepsy, (isolated) generalized tonic-clonic seizures) showed different patterns in comparison to controls [Betting et al., 2006]. However, no direct comparison between the groups has been reported.

Neurobiological Relevance of Reduced White Matter Connectivity

FA reduction (and MD increase) infers a reduction of directed, anisotropic fibers and/or their myelin sheet [Le Bihan et al., 2001] and has been found in several epileptic syndromes and after epilepsy surgery [Focke et al., 2008; Schoene-Bake et al., 2009; Yogarajah et al., 2010]. The increase in RD suggests that reduction of myelin may play a significant role in this context. The focus on the corpus callosum observed in generalized epilepsy syndromes could indicate a predominant disturbance of commissural connectivity. However, our study showed that other association tracts are also involved. Currently it is not clear whether these changes are cause or consequence of epilepsy. In a

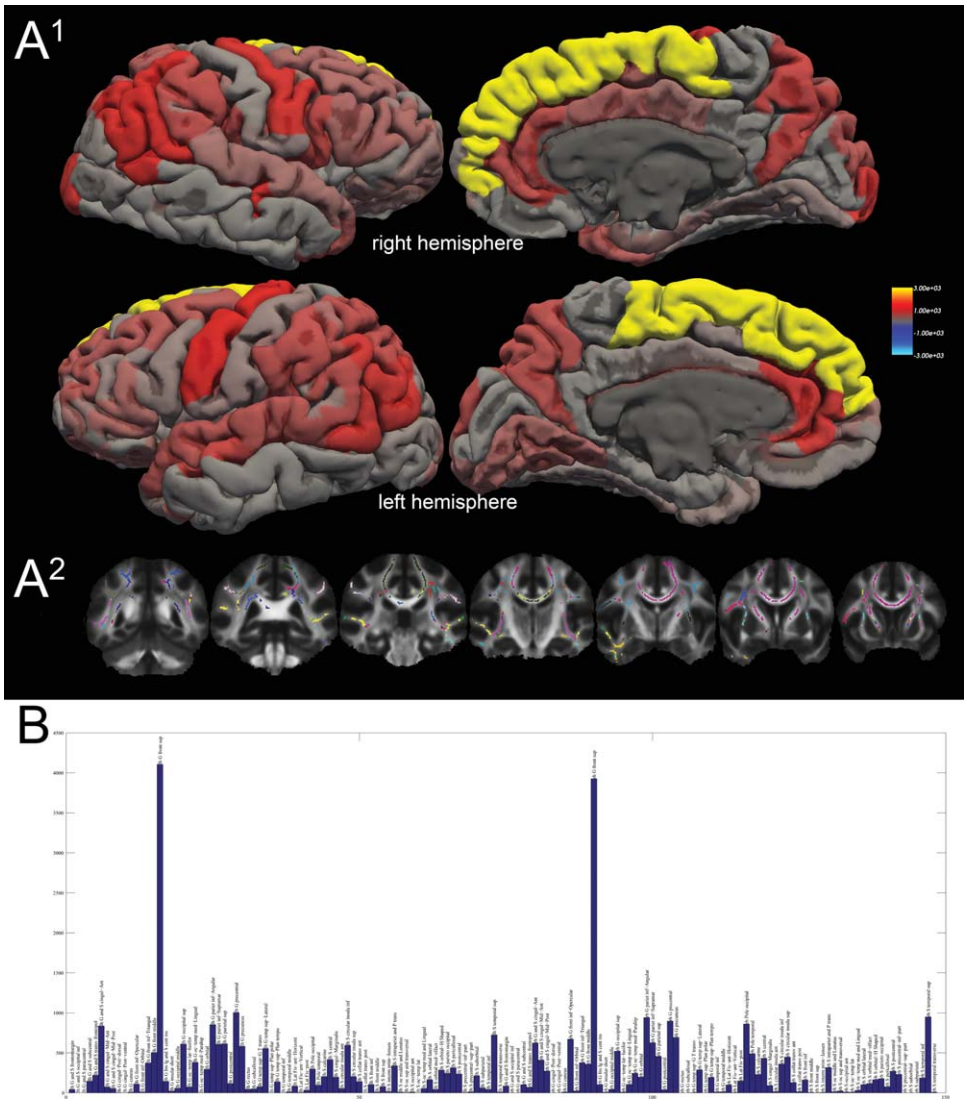

Figure 3.

Surface rendering of TBSS classification results. **A1**: Surface rendering of the absolute number of suprathreshold TBSS voxels projected onto the respective cortical region. The color scale represents values from 0 (transparent/red) to 3000 (opaque yellow). **A2**: Example slices of the target-based classified TBSS results (mode over all subjects). Each color represents a distinct cortical region (right and left hemisphere color codes are identical). **B**: The histogram displays the absolute voxel count (in TBSS normalized space) of all suprathreshold voxels of the FA TBSS comparison (patients [combined group] vs. controls) and the cortical regions of the Freesurfer (aparc.a2009s) atlas. The voxel count is shown on the *y* axis; the regions are binned on the *x* axis. A table of these results is also shown as Supporting Information Table 3. lh: left hemisphere, rh: right hemisphere, G: gyrus, S: sulcus, inf: inferior, sup: superior, med: medial, ant: anterior, post: posterior. A detailed explanation of the cortical regions is available in Destrieux et al. (2010).

comparison of supplementary motor area connectivity in JME and refractory frontal lobe epilepsy, only JME patients showed reduced FA in the corresponding tracts, supporting the notion that these alterations are not a consequence of epilepsy per se but are specific to generalized epilepsy [Vulliemoz et al., 2011]. Such observations may eventually challenge our view of epilepsy as a purely gray matter disease.

Limitations

Our patient selection and classification was based on clinical findings including repeated EEG and ultimately the clinical judgment of the treating physician. No genetic testing was available for the enrolled subjects. Thus, the lack of subtype specific MRI differences could be due to

suboptimal classification. Moreover, differentiation of IGE from frontal-lobe epilepsy is not always possible. Since all patients enrolled were diagnosed with idiopathic epilepsy invasive recordings were not available. A different substratification, e.g., based on genetic information may be preferable. However, currently (electro-)clinical classification remains the golden standard. Moreover, larger (sub-) group sizes could increase the statistical power to detect subtype specific DTI alterations. However, even with a liberal statistical threshold ($P < 0.001$ uncorrected) no significant differences were found. We also cannot exclude drug effects that are inevitable in a cross-sectional sample. To assess such effects a longitudinal study from the time of first diagnosis before commencement of drug treatment could be very interesting. To control other potentially confounding factors (age, sex, seizure freedom and epilepsy duration) we repeated the TBSS analysis with these factors as regressor of no interest (Supporting Information Figs. 1 and 2) showing no relevant change of the findings and generally low effect size of these confounds. A Freesurfer cortical thickness analysis showed no significant differences between patients and controls indicating that gray matter differences are limited in IGE/JME in concordance to the previous literature. The high rate of medically uncontrolled patients in our cohort is most likely explained by a sampling effect of a university referral center; as such, results may be different for other less refractory patients.

Summary

We show that patients with generalized epilepsy have severe alterations in DTI measures of structural connectivity. These include almost all major white matter tracts and may hint to a general pathophysiological process in IGE. Between clinically defined JME and undifferentiated IGE no significant DTI differences were found in the present sample. Further studies are needed to refine our current understanding of IGE subsyndromes possibly based on genetic classification and other imaging modalities.

DISCLOSURE

We confirm that we have read the Journal's position on issues involved in ethical publication and affirm that this report is consistent with those guidelines. N.K.F. served in an advisory board for GE Healthcare, received honoraria from GlaxoSmithKline and travel support from UCB/Schwarz, GlaxoSmithKline and Sanofi-Aventis. M.A.N. participated in advisory boards for, and received honoraria from UCB, GlaxoSmithKline, Eisai, and Neuroelectrics. H.L. has served on the scientific advisory boards for Eisai, GSK, Pfizer, UCB, and Valeant Pharmaceuticals International, received industry-funded travel costs from GSK, Pfizer, and UCB, received honoraria from Desitin, Eisai, GSK, Pfizer, and UCB, and received research support from Sanofi-Aventis. W.P. participated in advisory boards for, and received honoraria from GlaxoSmithKline, PPD Germany, UCB, Eisai, Allergan, Baxter, Cardinal Health Germany, CSL Behring, Desitin, Janssen Cilag, Otto Bock, Pfizer, Danish Agency for Science, EBS Technologies GmbH, Deutsches Stiftungszentrum and Talecris Biotherapeutics.

REFERENCES

Alexander A, Lee J, Lazar M, Field A (2007): Diffusion tensor imaging of the brain. Neurotherapeutics 4:316–329.

Behrens TEJ, Johansen-Berg H, Woolrich MW, Smith SM, Wheeler-Kingshott CAM, Boulby PA, Barker GJ, Sillery EL, Sheehan K, Ciccarelli O, Thompson AJ, Brady JM, Matthews PM (2003): Non-invasive mapping of connections between human thalamus and cortex using diffusion imaging. Nat Neurosci 6:750–757.

Berg AT, Berkovic SF, Brodie MJ, Buchhalter J, Cross JH, van Emde Boas W, Engel J, French J, Glauser TA, Mathern GW, Moshe SL, Nordli D, Plouin P, Scheffer IE (2010): Revised terminology and concepts for organization of seizures and epilepsies: Report of the ILAE Commission on Classification and Terminology, 2005-2009. Epilepsia 51:676–685.

Bernhardt BC, Rozen DA, Worsley KJ, Evans AC, Bernasconi N, Bernasconi A (2009): Thalamo-cortical network pathology in idiopathic generalized epilepsy: Insights from MRI-based morphometric correlation analysis. NeuroImage 46:373–381.

Betting LE, Mory SB, Li LM, Lopes-Cendes I, Guerreiro MM, Guerreiro CAM, Cendes F (2006): Voxel-based morphometry in patients with idiopathic generalized epilepsies. NeuroImage 32:498–502.

Bonilha L, Edwards JC, Kinsman SL, Morgan PS, Fridriksson J, Rorden C, Rumboldt Z, Roberts DR, Eckert MA, Halford JJ (2010): Extrahippocampal gray matter loss and hippocampal deafferentation in patients with temporal lobe epilepsy. Epilepsia 51:519–528.

Chahboune H, Mishra AM, DeSalvo MN, Staib LH, Purcaro M, Scheinost D, Papademetris X, Fyson SJ, Lorincz ML, Crunelli V, Hyder F, Blumenfeld H (2009): DTI abnormalities in anterior corpus callosum of rats with spike-wave epilepsy. NeuroImage 47:459–466.

Ciumas C, Savic I (2006): Structural changes in patients with primary generalized tonic and clonic seizures. Neurology 67:683–686.

Destrieux C, Fischl B, Dale A, Halgren E (2010): Automatic parcellation of human cortical gyri and sulci using standard anatomical nomenclature. NeuroImage 53:1–15.

Focke NK, Yogarajah M, Bonelli SB, Bartlett PA, Symms MR, Duncan JS (2008): Voxel-based diffusion tensor imaging in patients with mesial temporal lobe epilepsy and hippocampal sclerosis. NeuroImage 40:728–737.

Helms G, Ciumas C, Kyaga S, Savic I (2006): Increased thalamus levels of glutamate and glutamine (Glx) in patients with idiopathic generalised epilepsy. J Neurol Neurosurg Psychiatr 77: 489–494.

Huang W, Lu G, Zhang Z, Zhong Y, Wang Z, Yuan C, Jiao Q, Qian Z, Tan Q, Chen G, Liu Y (2011): Gray-matter volume reduction in the thalamus and frontal lobe in epileptic patients with generalized tonic-clonic seizures. J Neuroradiol 38:298–303.

Janz D (1985): Epilepsy with impulsive petit mal (juvenile myoclonic epilepsy). Acta Neurol Scand 72:449–459.

Jones NC, O'Brien TJ, Powell KL (2011): Morphometric changes and molecular mechanisms in rat models of idiopathic generalized epilepsy with absence seizures. Neurosci Lett 497:185–193.

Kim JH, Lee JK, Koh SB, Lee SA, Lee JM, Kim SI, Kang JK (2007): Regional grey matter abnormalities in juvenile myoclonic epilepsy: A voxel-based morphometry study. NeuroImage 37:1132–1137.

Kwan P, Brodie MJ (2000): Early identification of refractory epilepsy. New Engl J Med 342:314–319.

Le Bihan D, Mangin JF, Poupon C, Clark CA, Pappata S, Molko N, Chabriat H (2001): Diffusion tensor imaging: Concepts and applications. J Magn Reson Imag 13:534–546.

Liu M, Concha L, Beaulieu C, Gross DW (2011): Distinct white matter abnormalities in different idiopathic generalized epilepsy syndromes. Epilepsia 52:2267–2275.

Meencke HJ (1985): Neuron density in the molecular layer of the frontal cortex in primary generalized epilepsy. Epilepsia 26: 450–454.

Meencke HJ, Janz D (1984): Neuropathological findings in primary generalized epilepsy: A study of eight cases. Epilepsia 25:8–21.

O'Muircheartaigh J, Vollmar C, Barker GJ, Kumari V, Symms MR, Thompson P, Duncan JS, Koepp MJ, Richardson MP (2011): Focal structural changes and cognitive dysfunction in juvenile myoclonic epilepsy. Neurology 76:34–40.

Savic I, Lekvall A, Greitz D, Helms G (2000): MR spectroscopy shows reduced frontal lobe concentrations of *N*-acetyl aspartate in patients with juvenile myoclonic epilepsy. Epilepsia 41: 290–296.

Schoene-Bake J-C, Faber J, Trautner P, Kaaden S, Tittgemeyer M, Elger CE, Weber B (2009): Widespread affections of large fiber tracts in postoperative temporal lobe epilepsy. NeuroImage 46: 569–576.

Smith SM, Johansen-Berg H, Jenkinson M, Rueckert D, Nichols TE, Miller KL, Robson MD, Jones DK, Klein JC, Bartsch AJ, Behrens TE (2007): Acquisition and voxelwise analysis of multi-subject diffusion data with tract-based spatial statistics. Nat Protoc 2:499–503.

Song SK, Yoshino J, Le TQ, Lin SJ, Sun SW, Cross AH, Armstrong RC (2005): Demyelination increases radial diffusivity in corpus callosum of mouse brain. NeuroImage 26:132–140.

Vulliemoz S, Vollmar C, Koepp MJ, Yogarajah M, O'Muircheartaigh J, Carmichael DW, Stretton J, Richardson MP, Symms MR, Duncan JS (2011): Connectivity of the supplementary motor area in juvenile myoclonic epilepsy and frontal lobe epilepsy. Epilepsia 52:507–514.

Wheeler-Kingshott CAM, Cercignani M (2009): About "axial" and "radial" diffusivities. Magn Reson Med 61:1255–1260.

Woermann FG, Free SL, Koepp MJ, Sisodiya SM, Duncan JS (1999): Abnormal cerebral structure in juvenile myoclonic epilepsy demonstrated with voxel-based analysis of MRI. Brain: J Neurol 122 (Pt 11):2101–2108.

Yogarajah M, Focke NK, Bonelli SB, Thompson P, Vollmar C, McEvoy AW, Alexander DC, Symms MR, Koepp MJ, Duncan JS (2010): The structural plasticity of white matter networks following anterior temporal lobe resection. Brain: J Neurol 133: 2348–2364.